

ABSOLUTE BRANCHING RATIO NORMALIZATION FOR RARE  $\pi^+$  AND  
 $\mu^+$  DECAYS IN THE PIBETA EXPERIMENT

EMIL FRLEŽ  
(for the PIBETA Collaboration)

*University of Virginia, Department of Physics, Charlottesville, VA 22904, USA*  
*Tel: +1-434-924-6786, Fax: +1-434-924-4576, E-mail address: frlez@virginia.edu*

Received 27 October 2003; Accepted 26 April 2004  
Online 10 October 2004

We have used the PIBETA detector at the PSI for a precise measurement of rare pion and muon weak decays. We have collected a large statistical sample of (1)  $\pi^+ \rightarrow e^+\nu_e$ , (2)  $\pi^+ \rightarrow \pi^0 e^+\nu_e$ , (3)  $\pi^+ \rightarrow e^+\nu_e\gamma$ , (4)  $\mu^+ \rightarrow e^+\nu_e\bar{\nu}_\mu$ , and (5)  $\mu^+ \rightarrow e^+\nu_e\bar{\nu}_\mu\gamma$  decays. We have evaluated the absolute branching ratios for these processes by normalizing to the independently measured number of decaying  $\pi^+$ 's (or  $\mu^+$ 's). We discuss the mutual consistency of the preliminary results.

PACS numbers: 12.15.Hh, 13.20.Cz, 14.35.Bv, 14.40.Aq, 14.60.Ef UDC 539.12

Keywords: determination of CKM matrix elements, decays of pions and muons, properties of pions and muons

## 1. Introduction

The PIBETA Collaboration [1] at PSI has performed a series of high-precision measurements of rare pion and muon decays. We have used the PIBETA detector [2], a non-magnetic, segmented, pure CsI spherical calorimeter supplemented with a pair of cylindrical multi-wire proportional chambers for the charged particle tracking and a plastic veto hodoscope for the particle identification (Fig 1).

The primary goal of the experiment has been to determine the pion beta decay ( $\pi^+ \rightarrow \pi^0 e^+\nu_e$ ) branching ratio with  $\sim 0.5\%$  uncertainty, improving the precision of previous measurements by almost an order of magnitude [3]. Pion beta decay provides the theoretically most unambiguous means to study weak u-d quark mixing which directly tests quark-lepton universality and can thus constrain certain aspects of physics beyond the present Standard Model.

In the PIBETA experiment, a total of  $2.2 \cdot 10^{13}$   $\pi^+$  beam stops were recorded during several running periods spanning three years. The beam pions were counted

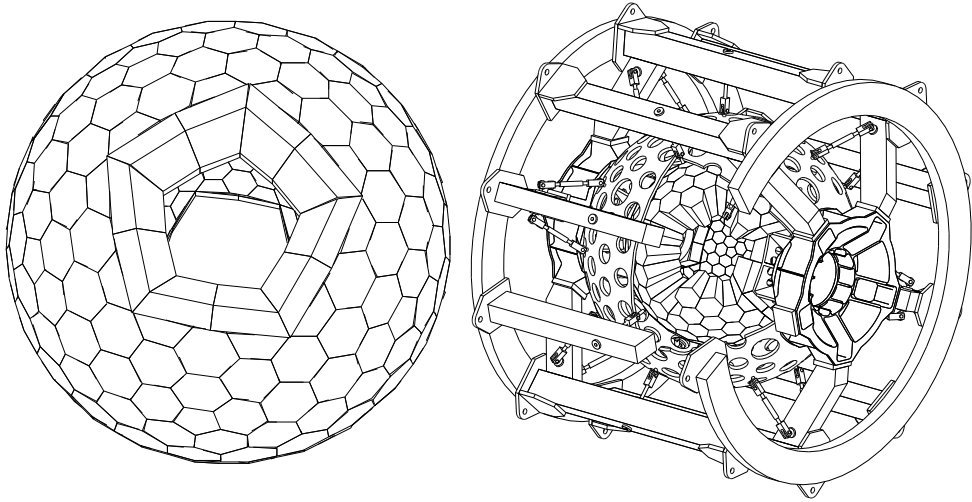


Fig. 1. The schematic drawing of the PIBETA detector. The left panel shows the geometry of the 240-module pure CsI shower calorimeter. The technical drawing of the assembled calorimeter is shown on the right.

by a tight fourfold coincidence between (1) a forward beam counter BC, (2) active degrader AD, (3) active target AT, and (4) rf accelerator signal. The non-pionic beam contamination determined by the time-of-flight method was small, 0.4%  $e^+$ 's and 0.2%  $\mu^+$ 's, respectively.

We have designed fast analog hardware triggers optimized to accept nearly all non-prompt processes contained in the calorimeter with an individual shower energy exceeding the Michel endpoint (high threshold  $\simeq 52$  MeV), while keeping the accidental rate to an acceptable level. We have also implemented an analogous set of electronically prescaled triggers with the low threshold of  $\simeq 5$  MeV. We have run with multiple simultaneous physics and calibration triggers at the  $\pi^+$  stopping rate of  $\sim 8 \cdot 10^5 \pi^+/s$  as well at a set of reduced beam fluxes down to  $4 \cdot 10^4 \pi^+/s$ , which was crucial for a reliable understanding of the detector response.

An experimental branching ratio  $R_i^{\text{exp}}$  for a particular pion (muon) decay can be evaluated using the expression

$$R_i^{\text{exp}} = \frac{N_i p_i}{N_{\pi/\mu} g_{\pi/\mu} A_i \tau_l \epsilon_{\text{PV}} \epsilon_{C_1} \epsilon_{C_2}}, \quad (1)$$

where  $N_i$  is the number of the detected events for the process  $i$ ,  $p_i$  is the corresponding hardware/software prescaling factor (if any),  $N_{\pi/\mu}$  is the number of the decaying  $\pi^+$ 's (or  $\mu^+$ 's),  $g_{\pi/\mu} = \int_{t_1}^{t_2} \exp(-t/\tau) dt$  is the  $\pi^+$  ( $\mu^+$ ) gate fraction,  $A_i$  is the detector acceptance incorporating the specific software cuts,  $\tau_l$  is the detector live time,  $\epsilon_{\text{PV}}$  is the plastic veto efficiency,  $\epsilon_{C_1}$  is the MWPC<sub>1</sub> chamber efficiency, and  $\epsilon_{C_2}$  is the MWPC<sub>2</sub> chamber efficiency. In our analysis we have used  $t_1 = 10$  ns

and  $t_2 = 130$  ns for the beginning and the end of integration range. The number of decaying  $\pi^+$ 's is equal to the number of  $\pi^+$ 's stopping in the target, corrected for a small loss due to hadronic interactions.

The total yield of the  $\pi^+ \rightarrow e^+\nu_e$  events was evaluated by two independent methods: (i) from the positron energy spectrum with the Michel background subtracted using the late-time events, and (ii) by fitting the positron timing spectrum. The consistency of these two methods was better than  $\sim 0.3\%$ . The  $\pi^+ \rightarrow e^+\nu_e$  positron energy lineshape and the charged particle tracking in the wire chambers and the CsI calorimeter are demonstrated in Fig. 2. Using Eq. (1) and normalizing to the number of decaying  $\pi^+$ 's, we find that the  $\pi^+ \rightarrow e^+\nu_e$  branching ratio is independent of the beam intensity. The average measured  $R_{\pi \rightarrow e\nu}$  value is

$$R_{\pi \rightarrow e\nu}^{\text{exp}} = [1.229 \pm 0.003(\text{stat}) \pm 0.007(\text{sys})] \cdot 10^{-4}, \quad (2)$$

in very good agreement with the theoretical predictions that incorporate radiative corrections [4].

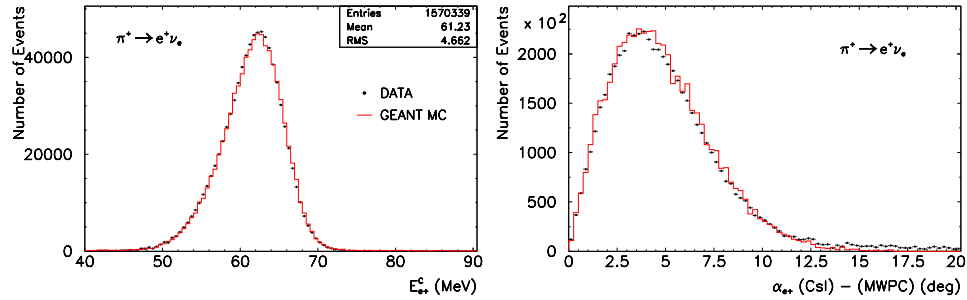


Fig. 2. A background-subtracted  $\pi^+ \rightarrow e^+\nu_e$  energy spectrum (left). A track definition using a difference in positron direction measured with MWPCs and the CsI calorimeter (right).

As demonstrated in Fig. 3, the  $\pi\beta$  data sample is exceedingly pure; the signal-

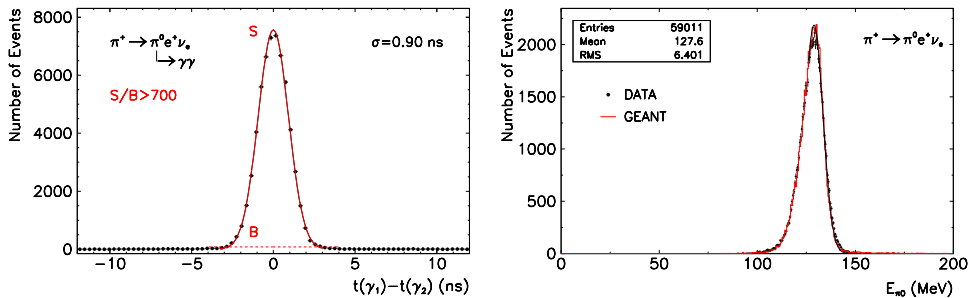


Fig. 3. The measured timing distribution between two coincident photons from  $\pi\beta$  decays (left). The reconstructed  $\pi^0$  energy spectrum compared with the Monte Carlo simulation (right).

to-background ratio is greater than 700. The analysis of the complete statistics in conjunction with the most stringent off-line cuts yielded  $\sim 60\,000$   $\pi\beta$  events. The preliminary branching ratio normalized to the number of decaying  $\pi^+$ 's is

$$R_{\pi\beta}^{\text{exp}} = [1.042 \pm 0.004(\text{stat}) \pm 0.007(\text{sys})] \cdot 10^{-8}. \quad (3)$$

A consistent  $R_{\pi\beta}$  value is obtained when using the known rate of the  $\pi^+ \rightarrow e^+\nu_e$  decays [4] for the absolute normalization. This method has the lower systematic uncertainties (ultimately  $\simeq 0.3\%$ ). We note that our experiment tests for the first time the calculation of the  $\pi\beta$  radiative corrections which stand at  $\text{RC}_{\pi\beta} \sim (+3.3 \pm 0.1)\%$  [5].

In its current phase, the PIBETA experiment has increased the existing world data set for  $\pi^+ \rightarrow e^+\nu_e\gamma$  process by more than 30-fold. Using one-arm and two-arm calorimeter triggers with high energy threshold, we have covered the radiative phase space regions dominated by the internal bremsstrahlung process as well as by the structure-dependent terms. The two-arm data set was restricted to  $e^+\text{-}\gamma$  coincident pairs for which both measured energies in the calorimeter were  $E_{e^+\gamma}^C > 51.7$  MeV, and for which the opening angle  $\theta_{e^+\gamma}^C > 40.0^\circ$  (phase space region A). The two one-arm data sets included coincidences for which the measured positron (photon)

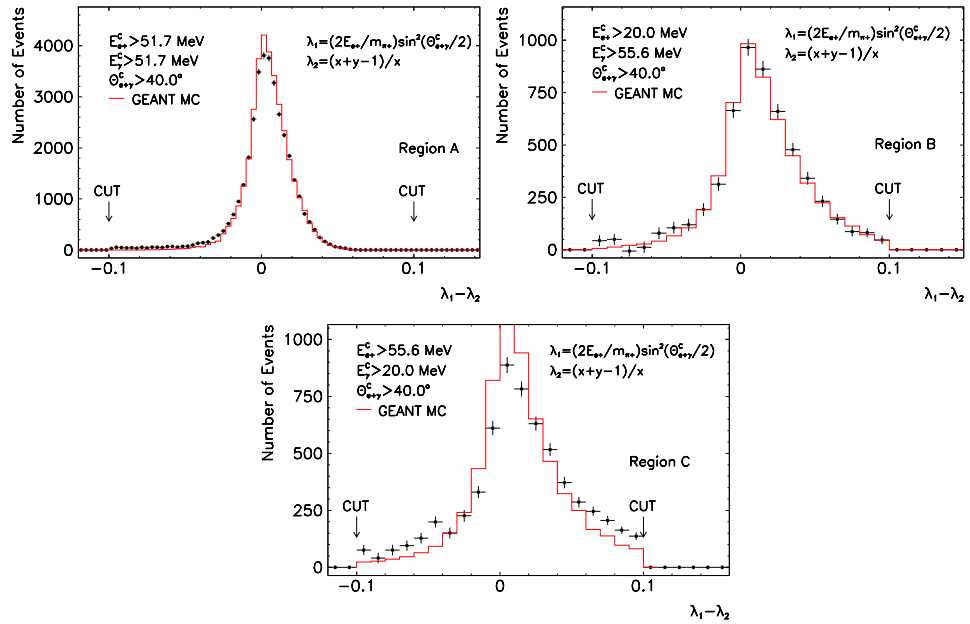


Fig. 4. Mismatch between the kinematic variable  $\lambda$  (see text) calculated in two alternative ways: (1) from measured positron and photon energies  $E_{e^+}^C$  and  $E_{\gamma}^C$  and (2) from measured positron energy  $E_{e^+}^C$  and the opening angle  $\theta_{e^+\gamma}^C$  (full markers). A Monte Carlo of predicted differences  $\lambda_1 - \lambda_2$  is shown as a full line histogram.

calorimeter energy was  $E_{e^+(\gamma)}^C > 20.0$  MeV, the photon (positron) energy  $E_{\gamma(e^+)}^C > 56.4$  MeV and their opening angle  $\theta_{e^+\gamma}^C > 40.0^\circ$  (phase space regions B and C). The reaction yields are calculated by subtracting out-of-time random coincidences from the events in the  $\pm 5$  ns signal region. The proper accounting was done for the unavoidable  $\pi\beta$  background. The purity of the final data set is demonstrated in Fig. 4.

TABLE 1. Comparison of preliminary experimental and SM-predicted branching ratios  $R_i$ . The absolute normalization is done using the number of decaying  $\pi^+$ 's or  $\mu^+$ 's.

Decay	PIBETA $R_i^{\text{exp}}$ Value	SM Theoretical $R_i^{\text{th}}$	Ref.
$\pi^+ \rightarrow e^+ \nu_e$	$(1.229 \pm 0.003 \pm 0.007) \cdot 10^{-4}$	$(1.2352 \pm 0.0005) \cdot 10^{-4}$	[4]
$\pi^+ \rightarrow e^+ \nu_e \gamma$ (A)	$(2.68 \pm 0.01 \pm 0.05) \cdot 10^{-8}$	$(2.55 \pm 0.01) \cdot 10^{-8}$	[8]
$\pi^+ \rightarrow e^+ \nu_e \gamma$ (B)	$(1.15 \pm 0.02 \pm 0.03) \cdot 10^{-7}$	$(1.43 \pm 0.01) \cdot 10^{-7}$	[8]
$\pi^+ \rightarrow e^+ \nu_e \gamma$ (C)	$(3.91 \pm 0.06 \pm 0.12) \cdot 10^{-7}$	$(3.78 \pm 0.01) \cdot 10^{-7}$	[8]
$\pi^+ \rightarrow \pi^0 e^+ \nu_e$	$(1.042 \pm 0.007 \pm 0.009) \cdot 10^{-8}$	$(1.039 \pm 0.001) \cdot 10^{-8}$	[5]
$\mu^+ \rightarrow e^+ \nu_e \bar{\nu}_\mu$	$0.971 \pm 0.003 \pm 0.010$	$0.988 \pm 0.005$	[9]
$\mu^+ \rightarrow e^+ \nu_e \bar{\nu}_\mu \gamma$	$(2.57 \pm 0.05 \pm 0.05) \cdot 10^{-3}$	$(2.584 \pm 0.001) \cdot 10^{-3}$	[7]

The corresponding partial branching ratios, extracted with the Monte Carlo minimization algorithm, are listed in Table 1. The fit corresponds to the ratio of weak axial vector to polar vector form factor  $\gamma \equiv F_A/F_V$  of

$$\gamma_{\text{exp}} = 0.429 \pm 0.008(\text{stat}) \pm 0.012(\text{sys}), \quad (4)$$

consistent with the present chiral symmetry phenomenology [6].

Phase space regions A and C agree well with the (V - A) model predictions and the CVC hypothesis; the region B indicates a  $\sim 22\%$  deficit in the number of observed  $\pi^+ \rightarrow e^+ \nu_e \gamma$  events.

We have simultaneously recorded a large set of radiative muon decay events  $\mu^+ \rightarrow e^+ \nu_e \bar{\nu}_\mu \gamma$  using the prescaled low threshold triggers (see Fig. 5). The experimental branching ratios in Table 1 are calculated from the event yields and numbers of decaying  $\mu^+$ 's in the conjunction with the Standard Model description [7] of the process and the Monte Carlo simulation of the detector response. For the phase space region limited by the positron and photon energies  $E_{e^+\gamma}^C > 20$  MeV and the particles' opening angle  $\theta_{e^+\gamma}^C > 20^\circ$  the measured radiative muon branching ratio is

$$R_{\mu \rightarrow e \nu \nu \gamma}^{\text{exp}} = [2.57 \pm 0.05(\text{stat}) \pm 0.05(\text{sys})] \cdot 10^{-3}, \quad (5)$$

agreeing with the prediction of the Standard Model [7]. Consistent results are again obtained when normalization is done with respect to the total number of detected

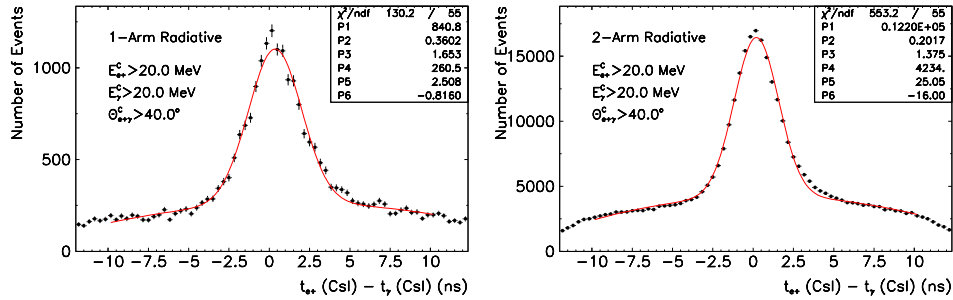


Fig. 5. Signal-to-background ( $S/B$ ) ratios for radiative muon events  $\mu^+ \rightarrow e^+ \nu_e \bar{\nu}_\mu \gamma$ . The  $S/B$  ratio for 1-arm calorimeter trigger (left) is 7.5. The 2-arm data (right) have the  $S/B$  ratio of 6.0.

Michel decays  $\mu^+ \rightarrow e^+ \nu_e \bar{\nu}_\mu$  (see Fig. 6). Moreover, the measured Michel decay branching ratio calculated using Eq. (1) is, within the experimental uncertainties, 100% (Table 1), indicating the excellent Monte Carlo simulation of the detector response as well as properly understood detector efficiencies.

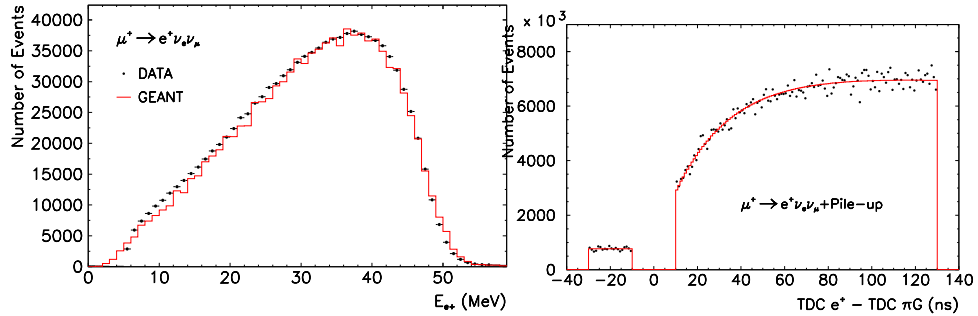


Fig. 6. The agreement between the measured  $\mu^+ \rightarrow e^+ \nu_e \bar{\nu}_\mu$  energy spectrum in the CsI calorimeter and the Monte Carlo simulation (left). The timing spectrum of  $e^+$ 's from  $\pi^+ - \mu^+ - e^+$  decay chain at the beam intensity of  $5 \cdot 10^4 \pi^+/s$  (right).

#### Acknowledgements

The PIBETA experiment has been supported by the National Science Foundation, the Paul Scherrer and the Russian Foundation for Basic Research. This material is based upon work supported by the National Science Foundation under Grant No. 0098758.

## References

- [1] D. Počanić et al., *PSI R-89.01 Experiment Proposal*, Paul Scherrer Institute, Villigen PSI, 1992.
- [2] PIBETA Collaboration Home Page, <http://pibeta.psi.ch/~pibeta/>.
- [3] W. K. McFarlane, L. B. Auerbach, F. C. Gaille, V. L. Highland, E. Jastrzembski, R. J. Macek, F. H. Cverna, C. M. Hoffman, G. E. Hogan, R. E. Morgado and R. D. Werbeck, *Phys. Rev. D* **32** (1985) 547.
- [4] W. J. Marciano, *Phys. Rev. Lett.* **71** (1993) 3629.
- [5] W. J. Marciano and A. Sirlin, *Phys. Rev. Lett.* **56** (1986) 22; W. Jaus, *Phys. Rev. D* **63** (2001) 053009(19); V. Cirigliano, M. Knecht, H. Neufeld and H. Pichl, *Eur. Phys. J. C* **27** (2003) 255.
- [6] B. R. Holstein, *Phys. Rev. D* **33** (1986) 3316.
- [7] W. Eichenberger, R. Engfer and A. van der Schaaf, *Nucl. Phys. A* **412** (1984) 412.
- [8] D. A. Bryman, P. Depommier and C. Leroy, *Phys. Rep.* **88** (1982) 151.
- [9] K. Hagiwara et al., *Review of Particle Physics*, *Phys. Rev. D.* **66** (2002) 1.

APSOLUTNO NORMIRANJE OMJERA GRANANJA RIJETKIH RASPADA  
 $\pi^+$  I  $\mu^+$  U EKSPERIMENTU PIBETA

Pomoću detektora PIBETA u PSI načinili smo precizna mjerenja rijetkih raspada piona i muona. Sakupili smo velik statistički uzorak za raspade (1)  $\pi^+ \rightarrow e^+\nu_e$ , (2)  $\pi^+ \rightarrow \pi^0 e^+\nu_e$ , (3)  $\pi^+ \rightarrow e^+\nu_e\gamma$ , (4)  $\mu^+ \rightarrow e^+\nu_e\bar{\nu}_\mu$  i (5)  $\mu^+ \rightarrow e^+\nu_e\bar{\nu}_\mu\gamma$ . Odredili smo apsolutne omjere grananja za te procese normirajući na neovisno mjerene raspade  $\pi^+$  (ili  $\mu^+$ ). Raspravljamo usklađenost početnih rezultata.